Metrologia

Absolute frequency measurement of an Yb optical clock at the 10^{-16} level using international atomic time

To cite this article before publication: Limeng Luo *et al* 2020 *Metrologia* in press https://doi.org/10.1088/1681-7575/abb879

IOP Publishing Journal Title
Journal **XX** (XXXX) XXXXXX https://doi.org/XXXX/XXXX

Absolute frequency measurement of an Yb optical clock at the 10^{-16} level using international atomic time

Limeng Luo[1], Hao Qiao[1], Di Ai[1], Min Zhou[1]*, Shuang Zhang[1], Sheng Zhang[1], Changyue Sun[1], Qichao Qi[1], Chengquan Peng[1], Taoyun Jin[1], Wei Fang[3], Zhiqiang Yang[2], Tianchu Li[2], Kun Liang[2]* and Xinye Xu[1,4]*

[1] State Key Laboratory of Precision Spectroscopy, East China Normal University, Shanghai 200241, People's Republic of China
[2] National Institute of Metrology, Beijing 100013, People's Republic of China
[3] China Jiliang University, Hangzhou 310018, People's Republic of China
[4] Shanghai Research Center for Quantum Sciences, Shanghai 201315, People's Republic of China

E-mail: mzhou@lps.ecnu.edu.cn; liangk@nim.ac.cn; xyxu@phy.ecnu.edu.cn

Received xxxxxx
Accepted for publication xxxxxx
Published xxxxxx

Abstract

We report on the absolute frequency measurement of the $6s^2\ {}^1S_0$–$6s6p\ {}^3P_0$ transition in ^{171}Yb with a fractional uncertainty of 7.3×10^{-16}. A GPS carrier phase frequency transfer was established between National Institute of Metrology (NIM) of China and East China Normal University (ECNU), which linked the optical frequency of the ECNU Yb1 clock to the second in the International System of Units (SI) through international atomic time. Frequency measurements were carried out in fifteen separate days with a total time over 3.8×10^5 seconds. The absolute frequency was determined to be 518 295 836 590 863.30(38) Hz. Our result is in good agreement with the recommended value in neutral Yb as a secondary representation of the SI second endorsed by the International Committee for Weights and Measures (CIPM).

Keywords: frequency metrology, optical clock, SI second, international atomic time

1. Introduction

Time and frequency are one pair of physical quantities that have the most measurable precision. Recent advances in some optical clocks have demonstrated the capability to reach frequency uncertainties at the 10^{-18} level [1-5]. Active investigations of optical clocks are being performed in many laboratories around the world, aiming to achieve better performance for precision frequency measurements, fundamental physics such as tests of relativity [6-8], and search of the time variation in fundamental constants [9, 10]. With the help of the optical frequency comb, the optical clock has also unlocked the potential in the research of frequency metrology, thereby stimulating a revision of the second in the International System of Units (SI) [11, 12].

The SI second is presently realized with the microwave transition between the ground hyperfine states in caesium 133. A roadmap for its redefinition using an optical transition frequency has been devised [13]. It is therefore essential to measure the absolute frequencies of candidate optical reference transitions with respect to the existing definition with comparable uncertinaties. For the future SI-related applications of optical clocks, especially assigned to regularly contribute to international atomic time (TAI), more optical

clocks have to be further consistent with uncertainties much lower than the best primary caesium standards, e.g., in the 10^{-18} regime, to overcome geopotential difficulties from the gravitational redshift.

Optical clocks could be realized either with single, trapped ion or with neutral atoms in an optical lattice. For optical lattice clocks, ^{171}Yb with nuclear spin $I = 1/2$ is one of the most popular candidates. Its unperturbed $6s^2\ ^1S_0$–$6s6p\ ^3P_0$ optical transition at 578 nm was endorsed by the International Committee for Weights and Measures (CIPM) as a secondary representation of the second [13]. To the best of our knowledge, there are five independent laboratories that have reported their absolute frequencies with respect to the ^{171}Yb clock transition [14-19]. Continual measurements are still being carried out on updating the absolute values towards much lower uncertainties. Prior to this work, systematic evaluation of our ^{171}Yb optical clock have been performed by synchronous comparison with the other nearly identical system Yb2 [20]. Here we further report on the absolute frequency measurement using a frequency link to TAI via National Institute of Metrology (NIM) of China, as shown in figure 1.

This paper is organized as follows. Section 2 describes the experimental system, including the ^{171}Yb frequency standard, the ultrastable laser and the optical comb for frequency measurement. Systematic shifts of the clock transition and their uncertainties are discussed in section 3. Section 4 shows the absolute frequency measurement. At the end we come to draw some conclusions.

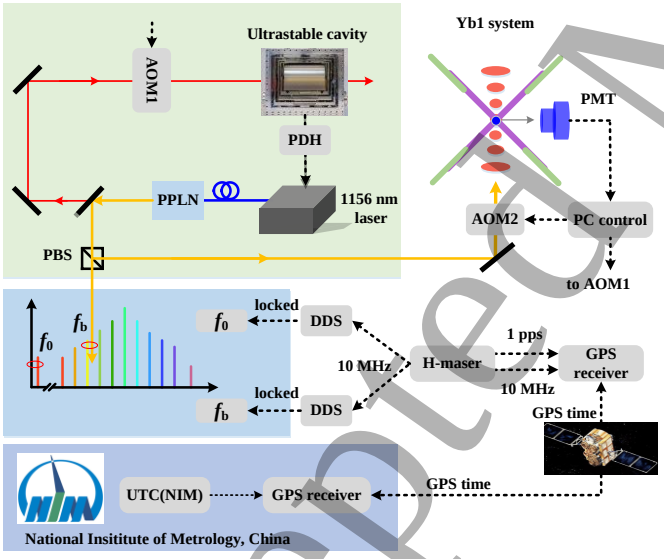

Figure 1. Simplified schematic of the experimental system. Shaded subsystems from top to bottom are the ultrastable laser, the optical frequency comb and the remote calibration site. AOM: acousto-optic modulator; PDH: Pound-Drever-Hall method; PMT: photomultiplier tube; PPLN: periodically poled lithium niobate; PBS: polarization beam splitter; f_0: carrier envelope offset frequency of the comb; f_b: beat note between the comb and the clock laser; DDS: direct digital synthesizer; GPS: global positioning system; UTC: universal coordinated time.

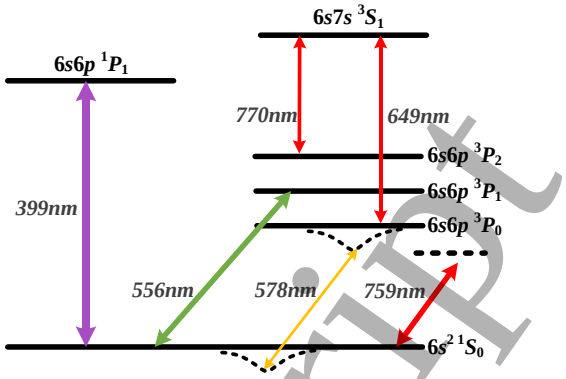

Figure 2. Partial level scheme for ^{171}Yb. The 399 nm radiation is used for two-dimensional collimation, Zeeman slowing, Doppler cooling and fluorescence detection. The 556 nm radiation is used for further Doppler cooling and state preparation. Both the 649 nm and 770 nm radiations are used for repumping. The 578 nm transition provides the optical reference for the ^{171}Yb frequency standard. The magic wavelength for the clock transition is 759 nm, at which the optical lattice provides the state independent trapping potential.

2. Experimental system

2.1 ^{171}Yb frequency standard

The Yb1 optical lattice clock at East China Normal University (ECNU) has been described elsewhere [20-22]. Here we only introduce the basic principle. The heart of the frequency standard is thousands of ^{171}Yb cold atoms that are trapped in an optical lattice. The $6s^2\ ^1S_0$–$6s6p\ ^3P_0$ electric dipole transition at 578 nm provides the optical reference for the frequency standard. Experimental access to this ultranarrow line (linewidth ~10 mHz [23]) is realized with the aid of Doppler- and recoil-free spectroscopy. Figure 2 shows ^{171}Yb energy levels relevant for laser cooling, trapping and state manipulation. Atoms are cooled to several microkelvin temperature in two successive MOTs that are based on the strong transition at 399 nm (linewidth ~29 MHz) and the weaker one at 556 nm (linewidth ~182 kHz), respectively. The one-dimensional tilted optical lattice, which is formed by retro-reflected laser beams at the magic wavelength of 759 nm, provides the recoil- and Stark-free environment for the clock transition interrogation.

Rabi excitation of the clock transition is performed with an ultrastable laser at 578 nm. To account for the excitation fraction, two lasers at 649 nm and 770 nm are used to pump atoms out of the excited $^3P_{0,2}$ states to the ground state for fluorescence detection [20]. For normal clock operation, the 578 nm laser is locked to the center of the atomic resonance by alternately interrogating two π components at each half maximum frequency.

2.2 Ultrastable laser

The ultrastable laser has been improved with respect to the one used in reference [20]. As shown in figure 1, the laser

source is generated from second harmonic generation (SHG) of an 1156 nm diode laser, by singly passing a periodically poled lithium niobate (PPLN) crystal waveguide. The fundamental light is frequency stabilized on a 30 cm long high finesse (~300 000) Fabry-Pérot (FP) cavity via the Pound-Drever-Hall (PDH) method [24]. The cavity spacer is made of ultralow-expansion (ULE) glass, which is suspended horizontally on four plastic support points in the vacuum chamber.

The zero coefficient of thermal expansion (CTE) point of the cavity is measured at around 33.1 ºC. Active temperature control of the cavity is implemented to maintain the target temperature. In order to reduce the vibration-induced cavity length fluctuation, the vacuum chamber and the optics for the PDH stabilization are placed on an active seismic-isolation platform, then enclosed in an anti-acoustic chamber. The thermal noise limited instability is predicted to be ~2×10^{-16}, which is much lower than that with the previous clock laser [20]. In fact, clock transition spectra with a Lorentzian linewidth of ~2 Hz have been observed. Further suppression of the different noise contributions and an elaborate evaluation are under consideration.

2.3 Optical frequency comb

As shown in figure 1, the clock frequency is measured with a commercial Er-doped femtosecond fiber frequency comb (Menlo Systems) with a repetition rate (f_r) of ~250 MHz. f_r is referenced to the ^{171}Yb stabilized clock laser by phase locking the beat note between the comb and the clock laser to a 35 MHz synthesizer. The rf synthesis, along with the rf distributor, is estimated to contribute an uncertainty of 1 part in 10^{-16}. The carrier envelope offset frequency of the comb, f_0, is phase-locked to an H-maser. The 10 MHz output of the H-maser is persistently calibrated by NIM. Counting error is assessed by measuring the 10 MHz maser signal, which is also used as the counter's external reference. This counting error contributes an uncertainty of as much as 1.6×10^{-17} on f_r, and also on the optical frequency. For data post-processing, computers need record the cavity-stabilized light frequency relative to the comb, and the frequency difference between the cavity and ytterbium atoms. Our comb was compared with another identical one at 1064 nm when both combs were locked to the Menlo 1 Hz linewidth laser system. The Allan deviation went below 1×10^{-18} after an averaging time of 2 000 seconds. Therefore, the measurement error from the optical frequency synthesis of the comb is expected to be < 1×10^{-18}.

3. Systematic frequency shifts

We investigate the uncertainty contributions from the systematic effects by synchronous comparison between two independent ^{171}Yb lattice systems under different physical conditions, and the details of the experiment are similar with our previously reported work [20]. Table 1 gives the systematic shifts and the uncertainty budget for the Yb1 optical lattice clock.

3.1 Lattice Stark shift

In our previous work [20], the systematic uncertainty is mainly limited by the ac Stark shift induced by the confining lattice light, which is the dominant effect from the electric dipole polarizability, leading to a linear shift with the trap depth. To minimize the shift, the lattice can be tuned to magic frequency at which the ground and excited clock states have identical electric dipole polarizability. However, in addition to the first-order scalar Stark shift, the nonlinear light shift induced multipolar polarizabilities and hyperpolarizability will prevent a complete cancellation of the light shift. In general, the induced lattice light shift can be written as $\Delta\upsilon_{\text{lattice}} = -\alpha U - \beta U^2$, where U is the trap depth in units of the lattice recoil energy E_r, and α and β are coefficients independent of U.

Table 1. Systematic evaluation of the ^{171}Yb optical clock.

Effect	Shift/mHz	Unc./10^{-17}
Lattice polarizability	539.1	8.10
Nonlinear lattice	-104.9	0.71
Clock laser Stark	0.06	<0.01
Collision	-241.8	6.29
Blackbody radiation	-1 263.1	4.71
2nd Zeeman	-77.2	5.81
Servo error	-5	0.87
Total	**-1 152.84**	**12.74**

In our experiment, the lattice-depth-dependent shifts are measured at different lattice frequencies from the synchronous comparison, in which the frequency of lattice laser of Yb1 is stabilized to the optical frequency comb that is referenced to the maser, and the other lattice laser is again locked to it. By changing the lattice laser frequency and the lattice intensity of Yb2, as figure 3 shows, we deduce the slope coefficient κ = 1.48×10^{-5} Hz/(E_r·MHz). The slope of the fitting lines is plotted in figure 4. Finally, the magic frequency is determined to be 394 798 299.0(4.7) MHz. Considering the normal operating conditions for the lattice laser at U = 606.6(6) E_r and 394 798 238.8 MHz, the lattice polarizability shift is estimated to be 539(42) mHz. From the known value of the hyperpolarizability coefficient reported in reference [25], the nonlinear shift is -104.9(3.7) mHz with an uncertainty of 7.8×10^{-18}.

3.2 Clock Stark shift

The interaction between the clock laser and the atoms during Rabi spectroscopy causes the Stark shift on the transition. We calculate this shift using the coefficient reported in reference [18]. In our experiment, the Rabi time is 300 ms and clock laser intensity is 0.004 mW·cm^{-2}. The shift is calculated as 0.06 mHz with an uncertainty of 0.012 mHz, which could be neglected in our measurement.

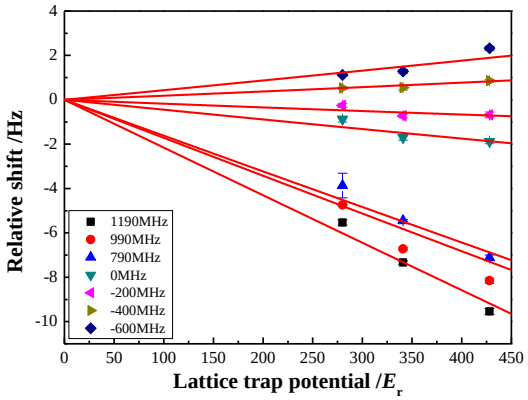

Figure 3. Frequency shifts of the clock transition as a function of lattice depth at different lattice frequencies. The points show experimental data while the red lines are quadratic fit.

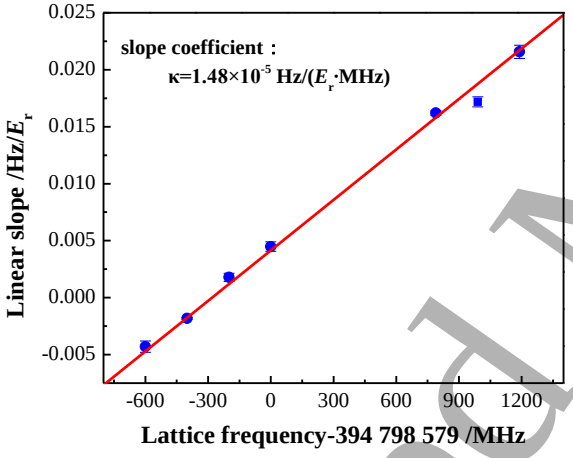

Figure 4. Magic lattice frequency determination. The linear slopes α fitted from figure 3 are plotted as a function of lattice frequency.

3.3 Zeeman effect

The first-order Zeeman effect is basically canceled by averaging the centre frequency of the two π components of the clock transition between m_F = ± 1/2 states. During one period of measurement, the background magnetic field is monitored with a three-dimensional digital magnetometer near the chamber, and we adopt a linear drift of 0.002(9) μT/h to estimate the first-order Zeeman shift. Considering the operating conditions of cycle time T_C = 795 ms and Zeeman splitting, the residual first-order Zeeman shift is estimated to be 0.002 mHz with an uncertainty less than 1 × 10^{-18}.

The second-order Zeeman shift depends on the square of the magnetic field that can not be canceled in this way. We determine the Zeeman shifts from synchronous comparison by measuring the clock frequency as a function of the magnetic field, as shown in figure 5. We fit the related data with the quadratic function and deduce a coefficient of b = -6.4(2.5) MHz/T^2. At the operational magnetic field of 0.1098 mT, the second-order Zeeman shift is estimated to be -77.2(30.1) mHz.

3.4 Collision shift

To evaluate the density dependent collision shift, we change the laser power for the Zeeman slower beam at 399 nm of Yb1 clock, which impacts the number of atoms loaded into the lattice without changing the trapping conditions. The atom number is measured by the use of integrated fluorescence signals of the 399 nm probe light by an intensified CCD (ICCD). We obtain the dependence of the clock frequency shift $\Delta\upsilon$ on the atom number N with a linear function as $\Delta\upsilon$ = -3.104 × 10^{-4} Hz·N. The atom number is calibrated to be 779(105), so the shift is estimated to be -241.8(32.6) mHz.

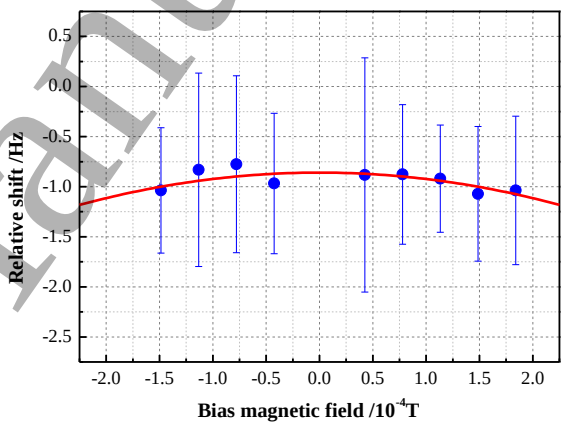

Figure 5. Measuring the second-order Zeeman shift versus external magnetic field. Experimental data are fitted with quadratic function for which b is -6.4(2.5) MHz/T^2.

3.5 Blackbody radiation (BBR)

Blackbody radiation (BBR) from the finite-temperature surroundings shifts the clock transition, and the value of the shift can reach the Hertz level for the normal experiment condition. To evaluate the BBR shift, it is important to acquire the complete knowledge of the temperature around the atoms. In our experiment, we use seven calibrated PT100 sensors to measure the temperature on the outer surface of chamber and a sensor to measure the air temperature above the chamber. By making the finite-element radiation analysis on the chamber with the temperature data, we could get the temperature around the cold ytterbium atoms [26]. In our calculation model, there are three contributions that need to be considered. The first is the temperature from the outside of the chamber and through the chamber windows, which leads the shift of -

26.9 mHz. The second contribution comes from the inner surface of the chamber, and the shift is -1 235.3 mHz. The third comes from the heated atomic oven, and the shift is -0.84 mHz. Therefore, the total BBR shift is estimated to be -1 263.1 mHz with an uncertainty of 4.7×10^{-17}.

3.6 Servo error and minor shifts

The servo error shift is calculated by taking the average of the error signal measured during the campaign. The frequency instability is determined from the Allan standard deviation that gives a fractional uncertainty of 8.6×10^{-18}. For some other systematic effects, such as the residual Doppler shift, are estimated to be negligibly small within our frequency measurement uncertainty. The fractional uncertainty contributed by phase-stabilized fiber links between the 578 nm laser and the atoms is less than 1×10^{-18} after 1000 s.

4. Absolute frequency measurement

A schematic of the frequency calibration link is depicted in figure 6. On the one hand, the Yb1 clock is measured versus the H-maser, which acts as the fly-wheel clock to be compared with the universal coordinated time of NIM (UTC(NIM)), using a global positioning system (GPS) carrier phase frequency transfer. The GPS link between NIM and ECNU was constructed by locating two time transfer equipments separately at both sites including one Piketime TTS5 receiver at ECNU and one Dicom GTR50 receiver at NIM. In this way, the optical clock can be compared to UTC(NIM). On the other hand, UTC(NIM) is traced to UTC, thereby linking the TAI, as TAI has the same scale interval with UTC. The deviation between the TAI and the SI is published in the Circular T by Bureau International des Poids et Mesures (BIPM) every month. Therefore, the caesium fountain clock NIM5 at NIM is used to reproduce the SI second and the optical clock could remotely be traced to the SI second via NIM5.

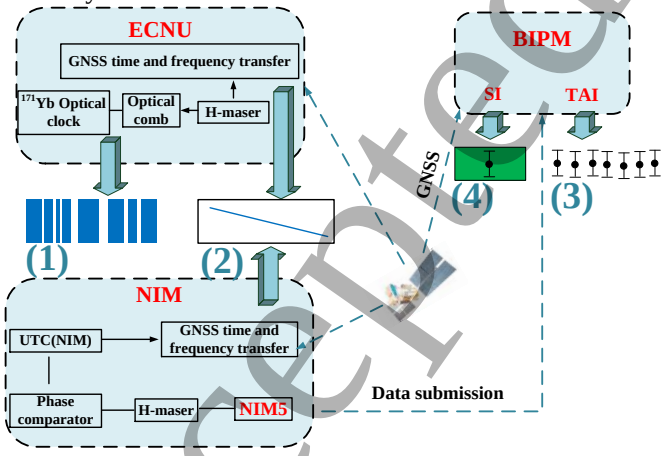

Figure 6. Schematic of frequency calibration of the ECNU Yb1 optical lattice clock via NIM. (1) Optical clock frequency measured with comb with respect to the H-maser, (2) link data between ECNU and NIM, (3) time difference data between UTC(NIM) and UTC reported in the Circular T, (4) absolute frequency acquisition.

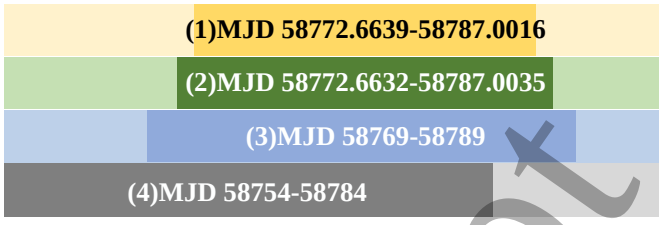

Figure 7. Actual time spans for four types of measurements. (1) Optical clock frequency measurement with respect to the H-maser, (2) H-maser measurement with respect to UTC(NIM), (3) UTC-UTC(NIM) measurement, (4) duration of the TAI scale interval *d*.

In the tracing link, there are four kinds of data that must be used for the computation, including optical clock frequency data measured with respect to the H-maser by the comb, comparison data between the H-maser and UTC(NIM), UTC-UTC(NIM) data and the duration of the TAI scale interval *d*. The corresponding time spans for four types of measurement data are shown in figure 7.

The frequency of the optical clock transition was continuously measured for about fifteen days (MJD 58 772 to 58 787) in October 2019 at ECNU. The ^{171}Yb lattice clock was operated several hours per day, specifically at night as periodically as possible from MJD 58 772.663 9 to MJD 58 787.001 6. There are 384 196 effective points and 1 238 782 time epochs in total. The average relative frequency difference for the optical comparison to its flywheel H-maser is calculated as 518 295 836 587 542.3 Hz using the optical frequency data in figure 8.

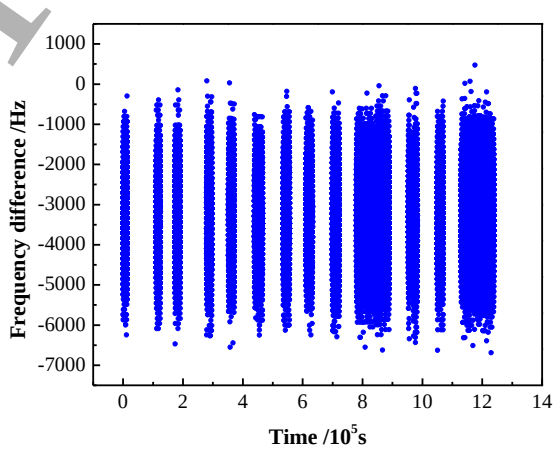

Figure 8. ^{171}Yb optical clock frequency measured with the optical comb.

Based on the measurement data of the optical clock referenced to the H-maser, the noise parameters for the H-maser could be estimated with τ in seconds as white phase noise $1.67 \times 10^{-12}\ \tau^{-1}$, flicker phase noise $4.72 \times 10^{-13}\ \tau^{-1}$, white frequency noise $2.81 \times 10^{-13}\ \tau^{-1/2}$, flicker frequency noise 3.38×10^{-15} and random walk frequency noise $2.77 \times 10^{-17}\ \tau^{-1/2}$. With these parameters, the data for these days were simulated in term of the principles in references [27-30]. The uncertainty

can be estimated to be 4.89 × 10^{-16} using the difference between the averaged frequency in 384 196 measurements for the corresponding time epochs in the simulated data and the averaged frequency for all the simulated data.

To avoid the uncertainty from different time spans between the clock frequency measurement versus the H-maser and H-maser measurements referenced to UTC(NIM), the data in the GPS carrier phase link between ECNU and NIM with roughly the same period are used. In this part, the effect from the frequency drift of H-maser should be considered in the calculation. By a least-squares fitting to the data in figure 9, the uncertainty from the frequency drift of H-maser is 8.6 × 10^{-17}.

In our measurement, the largest frequency correction of more than 3 kHz comes from the frequency offset of the H-maser. During the MJD 58 772.663 2 to 58 787.003 5, the frequency differences between the H-maser at ECNU and UTC(NIM) were measured with the precise point position (PPP) processing service, which is essentially the same method as used in TAI computation. As shown in figure 9, the fractional frequency offset of the flywheel clock from UTC(NIM) is calculated to be 6.403 718 310 948 821 × 10^{-12}.

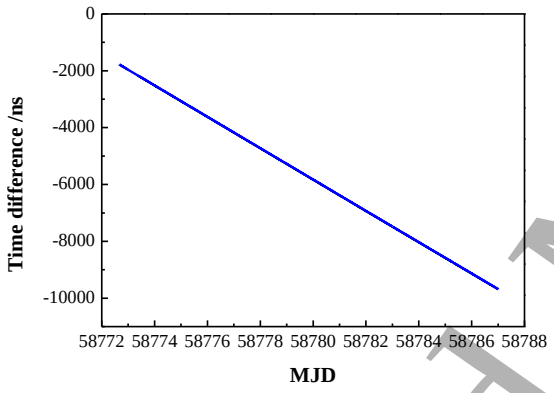

Figure 9. Link data between ECNU and NIM. The time difference, UTC(NIM)-H-maser(ECNU), is measured between the 1 pps signals from two sites.

As mentioned above, since the ^{171}Yb optical clock at ECNU in Shanghai is about 1 200 kilometers away from NIM, we used the precise frequency link by GPS carrier phase with a low uncertainty. The time link stability is classically evaluated to be 0.3 ns as u_A of UTC-UTC(*k*) by BIPM [31, 32] in UTC computation every month. It is finally taken into account in our final uncertainty evaluation for the frequency measurement.

Inspired by the idea from BIPM [33], in the computation of UTC, any laboratory can be considered as a virtual "additional laboratory" that could be included in the Circular T but would not change the existing values. That is to say, specifically, the ECNU holding the Yb lattice clock to be calibrated could be regarded as one virtual laboratory participating in the TAI cooperation and the link uncertainty from the link between the remote laboratory ECNU and the real TAI laboratory NIM could be canceled out.

The results of the frequency link between the local time reference UTC(NIM) and UTC can be found in Circular T, which is published on BIPM web page and calculated for a 5-day interval. From Circular T No.382 [31] and No.383 [32], five time differences, 4.5 ns, 3.9 ns, 3.5 ns, 2.6 ns and 1.7 ns between MJD 58 769 and 58 789 have been involved in the computation. The frequency difference between UTC(NIM) and UTC is calculated to be 1.620 × 10^{-15}. Based on the measurement data of the UTC(NIM) referenced to one H-maser of NIM via dual mixing time difference device (DMTD), the noise parameters for the UTC(NIM) could be estimated as white phase noise 1.70 × 10^{-12} τ^{-1}, flicker phase noise 4.52 × 10^{-13} τ^{-1}, white frequency noise 8.33 × 10^{-13} $\tau^{-1/2}$, flicker frequency noise 2.56 × 10^{-15} and random walk frequency noise 8.89 × 10^{-18} $\tau^{1/2}$. With these parameters, the data for twenty days corresponding to MJD 58 769 and MJD 58 789 from Circular T, the 5 760 measurements were simulated in 300 s. The uncertainty can be estimated as 1.91 × 10^{-16} using the difference between the averaged frequencies for the measurements in (2) and (3) shown in figure 7.

For the tracing from TAI to the SI second, the *d* value is -3.5 × 10^{-16}, which is calculated between MJD 58 754 00:00:00-58 784 00:00:00 from the Circular T as well, with uncertainty of 1.4 × 10^{-16}. The principle for the estimation of this uncertainty is just the same as that in the last paragraph. The noise parameters for the UTC could be given by BIPM as white frequency noise 1.4 × 10^{-15} $\tau^{-1/2}$, flicker frequency noise 3 × 10^{-16} and random walk frequency noise 2 × 10^{-17} $\tau^{1/2}$. With these parameters, during MJD 58 754 and MJD 58 784, the seven measurements were simulated in 86 400 × 5 s. The uncertainty can be estimated as 2.88 × 10^{-16} using the difference between the averaged frequencies for the measurements in (3) and (4) shown in figure 7.

We adopt the method used in reference [34] to evaluate the gravitational redshift. The height of Yb atoms in an optical lattice from the earth ellipsoid (WGS84) is measured to be 3.1(3) m from the GPS antenna data and orthometric height levelling. The geoid undulation is obtained by the Earth Gravitational Model (EGM2008). Taking the bias by a dynamic part attributed to the tidal effect as an additional uncertainty, the gravitational shift is estimated to be 0.175(20) Hz.

Recent synchronous comparison with the Yb2 system basically shows the Yb1 optical lattice clock has a fractional instability of 4.60 × 10^{-16} $\tau^{-1/2}$ [35]. Therefore, a total record length of the measurement leads to a statistical uncertainty less than 1 × 10^{-18}. Since the fluctuation of the H-maser is much more than the inaccuracy of the Yb system, the uncertainty of the absolute frequency measurement is determined by the evaluation of the H-maser frequency and the link, we list all significant frequency shifts and their uncertainties in table 2.

As summarized in table 2, the absolute frequency of the clock transition relative to the SI second is 518 295 836 590 863.30(38) Hz. The result is compared with previous measurements [14-19, 34, 36-39] in figure 10. The measured absolute frequency in this work agrees well with the CIPM recommendation in 2017 [40].

5. Conclusion and perspectives

In conclusion, we have described the absolute frequency measurement in the ^{171}Yb optical clock. The measurement is referenced to the SI second through the TAI by two main steps: the frequency link between our lab and UTC(NIM), and the frequency link between UTC(NIM) and the TAI. The absolute frequency is determined to be 518 295 836 590 863.30(38) Hz with an unceratainty of 7.3×10^{-16}. We expect this value will contribute to the determination of a new recommended values for the secondary representations of the second by the CIPM.

Table 2. Uncertainty budget for the absolute frequency measurement of the clock transition in ^{171}Yb.

Unc. source	Contribution	Unc./10^{-16}
Yb1(ECNU)	syst. (Table 1)	1.27
	statistical	< 0.01
	clock dead time	4.89
Optical comb	optical frequency synthesis	< 0.01
	rf distribution and synthesis	1.00
	counter	0.16
H-maser(ECNU)-UTC(NIM)-TAI	H-maser drift	0.86
	link with TAI	3.43
	UTC(NIM) extrapolation	1.91
TAI-SI	*d* estimation	1.4
	TAI extrapolation	2.88
Gravitational redshift		0.386
Total		**7.29**

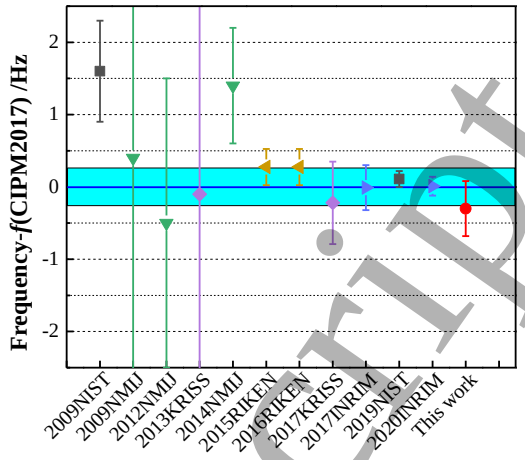

Figure 10. Absolute frequency values of ^{171}Yb clock transition measured by different laboratories [14-19, 34, 36-39]. The blue solid line and the shaded region represent the CIPM recommended value and its uncertainty, respectively [40]; *f*(CIPM2017) = 518 295 836 590 863.60(26) Hz.

Acknowledgements

We thank Gérard Petit for his help on data processing and fruitful suggestions on the calculation of the absolute frequency. This work is supported by National Key Research and Development Program of China (NO.2016YFA0302103, NO.2017YFF0212003, NO.2016YFB0501601), Shanghai Municipal Science and Technology Major Project (NO.2019SHZDZX01), National Natural Science Foundation of China (NO.11134003), Shanghai Excellent Academic Leaders Program (NO.12XD1402400).

Reference

[1] Chou C W, Hume D B, Koelemeij J C J, Wineland D J and Rosenband T 2010 *Phys. Rev. Lett.* **104** 070802
[2] Ushijima I, Takamoto M, Das M, Ohkubo T and Katori H 2015 *Nat. Photonics* **9** 185-9
[3] Nicholson T L et al 2015 *Nat. Commun.* **6** 6896
[4] Huntemann N, Sanner C, Lipphardt B, Tamm C and Peik E 2016 *Phys. Rev. Lett.* **116** 063001
[5] McGrew W F et al 2018 *Nature* **564** 87-90
[6] Chou C W, Hume D B, Rosenband T and Wineland D J 2010 *Science* **329** 1630-3
[7] Delva P et al 2017 *Phys. Rev. Lett.* **118** 221102
[8] Takamoto M, Ushijima I, Ohmae N, Yahagi T, Kokado K, Shinkai H and Katori H 2020 *Nat.Photonics* accepted
[9] Huntemann N, Lipphardt B, Tamm C, Gerginov V, Weyers S and Peik E 2014 *Phys. Rev. Lett.* **113** 210802
[10] Godun R M, Nisbet-Jones P, Jones J, King S, Johnson L, Margolis H, Szymaniec K, Lea S, Bongs K and Gill P 2014 *Phys. Rev. Lett.* **113** 210801
[11] Riehle F 2015 *C. R. Phys.* **16** 506-15
[12] Bize S 2019 *C. R. Phys.* **20** 153-68
[13] Riehle F, Gill P, Arias F and Robertsson L 2018 *Metrologia* **55** 188-200

[14] Nemitz N, Ohkubo T, Takamoto M, Ushijima I, Das M, Ohmae N and Katori H 2016 *Nat.Photonics* **10** 258-61
[15] Akamatsu D, Yasuda M, Inaba H, Hosaka K, Tanabe T, Onae A and Hong F L 2014 *Opt. Express* **22** 7898-905
[16] Park C Y et al 2013 *Metrologia* **50** 119-28
[17] Yasuda M et al 2012 *Appl. Phys. Express* **5** 102401
[18] Lemke N D et al 2009 *Phys. Rev. Lett.* **103** 063001
[19] Pizzocaro M, Thoumany P, Rauf B, Bregolin F, Milani G, Clivati C, Costanzo G A, Levi F and Calonico D 2017 *Metrologia* **54** 102-12
[20] Gao Q et al 2018 *Sci. Rep.* **8** 8022
[21] Chen N et al 2013 *Chin. Phys. B* **22** 090601
[22] Zhang X et al 2015 *Laser Phys. Lett.* **12** 025501
[23] Porsev S G, Derevianko A and Fortson E N 2004 *Phys. Rev. A* **69** 021403
[24] Black E D 2001 *Am. J. Phys.* **69** 79–87
[25] Brown R C et al 2017 *Phys. Rev. Lett.* **119** 253001
[26] Xu Y L, Xu X Y 2016 *Chin. Phys. B* **25** 103202
[27] Hidekazu H and Tetsuya I 2015 *Jpn. J. Appl. Phys.* **54** 112401
[28] Hidekazu H, Gérard P, Fumimaru N, Yuko H and Tetsuya I 2017 *Opt. Express* **25** 8511-23
[29] King S A, Godun R M, Webster S A, Margolis H S, Johnson L A M, Szymaniec K, Baird P E G and Gill1 P 2012 *New J. Phys.* **14** 013045
[30] Dai-Hyuk Y, Marc W and Thomas E P 2007 *Metrologia* **44** 91
[31] ftp://ftp2.bipm.org/pub/tai//CircularT/cirthtm/cirt.382.html
[32] ftp://ftp2.bipm.org/pub/tai//Circular-T/cirthtm/cirt.383.html
[33] Petit G and Panfilo G 2018 *European Frequency & Time Forum* 185–7
[34] Kim H, Heo M S, Lee W K, Park C Y, Hong H G, Hwang S W and Yu D H 2017 *Jpn. J. Appl. Phys.* **56** 050302
[35] Ai D et al 2020 *Chin. Phys. B* accepted
[36] Kohno T, Yasuda M, Hosaka K, Inaba H, Nakajima Y and Hong F L 2009 *Appl. Phys. Express* **2** 072501
[37] Takamoto M et al 2015 *C. R. Phys.* **16** 489-98
[38] Mcgrew W F et al 2019 *Optica* **6** 448-54
[39] Pizzocaro M, Bregolin F, Barbieri P, Rauf B, Levi F and Calonico D 2020 *Metrologia* **57** 035007
[40] Bureau International des Poids et Mesures 2017 *Consultative Committee for Time and Frequency (CCTF) report of the 21st meeting to the International Committee for Weights and Measures*